ACS APPLIED MATERIALS & INTERFACES

Letter

www.acsami.org

UV-Assisted Modification and Removal Mechanism of a Fluorocarbon Polymer Film on Low-*k* Dielectric Trench Structure

Tamal Mukherjee,[†] Seare A. Berhe,[†] Arindom Goswami,[†] Oliver Chyan,*[,†] Kanwal Jit Singh,[‡] and Ian Brown[§]

[†]Department of Chemistry, Interfacial Electrochemistry and Materials Research Lab, University of North Texas, Denton, Texas 76203, United States

[‡]Components Research, Intel Corporation, 2501 NW 229th Avenue, Hillsboro, Oregon 97203, United States

[§]Technology Development Center, Tokyo Electron U.S. Holdings, Inc., 2400 Grove Boulevard, Austin. Texas 78704, United States

Supporting Information

ABSTRACT: In this study, we report the first chemical characterization of a plasma-deposited model fluoropolymer on low-*k* dielectric nanostructure and its decomposition in UV/O_2 conditions. Carbonyl incorporation and progressive removal of fluorocarbon fragments from the polymer were observed with increasing UV (≥230 nm) irradiation under atmospheric conditions. A significant material loss was achieved after 300 s of UV treatment and a subsequent wet clean completely removed the initially insoluble fluoropolymer from the patterned nanostructures. A synergistic mechanism of UV light absorption by carbonyl chromophore and oxygen incorporation is proposed to account for the observed photodegradation of the fluoropolymer.

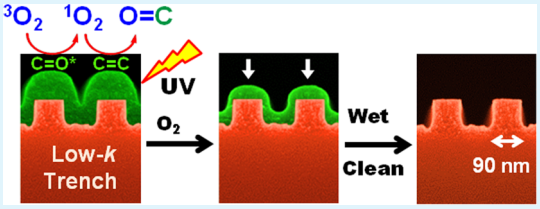

KEYWORDS: *low-k dielectrics, fluorocarbon polymer, postetch residue removal, UV irradiation, photosensitization, singlet oxygen*

In advanced copper interconnect design, porous carbon-doped silicon oxide (CDO) low-*k* dielectric materials replace traditional dense oxide as the interlayer dielectrics (ILD) to further reduce resistance-capacitance (RC) time delays. However, porosity induced to lower the dielectric constant of the ILD has the undesirable side effect of compromising its mechanical and chemical stability.[1] As a result, these materials are more susceptible to the plasma-induced damages caused by reactive-ion etching processes. To maintain accurate profile control and minimize damage to the dielectric, a standard solution path employed in the industry is to use heavily polymerizing plasma chemistries to deposit thin fluoropolymers on all surfaces during the etching step.[2] Although these thin polymers help in mitigating plasma-induced damage, they are often difficult to dissolve and/or remove in the subsequent removal step. These polymers must be selectively and completely removed prior to deposition of subsequent layers to avoid contamination, achieve good adhesion and coverage. Typically, a combination of dry photoresist strip (O_2, H_2, N_2, He, Ar plasma) followed by a wet clean method (aqueous/semiaqueous fluoride-containing solutions or amine-based alkaline solution mixtures) is used for complete fluoropolymer removal.[3] Both dry plasma strip and wet chemical treatments induce degradation of porous low-*k* dielectrics by carbon depletion, material densification, silanol formation and water absorption. An alternative approach involves structural modification and introduction of labile functional groups into these otherwise chemically inert fluoropolymer films by UV irradiation. Improved cleaning efficiency was observed for various wet removal methods each following a UV/O_2 irradiation on model fluorocarbon polymer (MFP) films deposited on blanket or 4 × 4 cm^2 checkerboard dielectric patterned structures.[4−8] Necessary external conditions for complete removal of fluorocarbon films were identified as a high UV dose and high O_2 density ensuing significant decrease of fluorine content, incorporation of oxygen, increased surface hydrophilicity and a concomitant decrease in fluoropolymer film thickness. Le et. al proposed that C═C and in particular C−O saturated bonds in MFP play key role for light absorption and subsequent bond scission process.[6] Although etch/cleans study on blanket and large dielectric structure reveal initial helpful information, further optimization of fabrication process requires systematic characterization on a manufacturing relevant dielectric trench nanostructure. (see the Supporting Information, Figure S1)

Using sensitive Fourier transform infrared (FTIR) metrology, we have recently identified key bonding transformations during various IC manufacturing steps for porous low-*k* dielectrics fabrication.[9−11] For example, FTIR spectroscopy helped to establish the chemical bonding structure of model fluorocarbon polymer films deposited on trench structures patterned in porous low-*k* dielectric and evaluate plasma-induced dielectric damages on high aspect ratio trench patterns.[9,10] With functional group-specific chemical derivatiza-

Received: December 16, 2014
Accepted: February 13, 2015
Published: February 13, 2015

DOI: 10.1021/am508734b
ACS Appl. Mater. Interfaces 2015, 7, 5051−5055

tion, the MFP coating on low-*k* trench structure was determined to consist of amorphous cross-linked fluorinated backbone decorated with fluorinated olefins and carbonyl functionalities.[9] In this paper, we investigated UV-induced chemical modification and subsequent semiaqueous wet removal of ca. 28 nm MFP films deposited on 90 nm critical dimension (CD) 180 nm pitch low-*k* dielectric trench lines by FTIR, XPS and SEM. Based on new chemical bonding transformation insights obtained and control experiments done, we propose possible mechanistic explanations for the UV-assisted structural modifications and observed material removal of MFP films under oxygen atmosphere.

Trench patterns consisting of 90 nm lines were patterned on CDO dielectric film (*k*-value <2.5) deposited on Si substrate using CH_2F_2/CF_4 plasma chemistry by a LAM Research 2300 Exelan etch platform. After cleaning with a dielectrics-compatible solvent, $CHF_3/C_4F_8/Ar$ plasma treatment was optimized to deposit a conformal MFP film (~28 nm) on CDO trench patterns with minimal dielectric etching. Proprietary experimental hardware built by Tokyo Electron consisting of a broadband light source (160−1100 nm) with specific filters to block UV emissions below 230 nm was used to irradiate samples in atmospheric conditions. Post-UV exposure, the samples were subsequently cleaned at 60 °C for 4 min in a proprietary cleaning solvent closely mimicking industrial cleaning standards. Transmission IR spectra were collected at 4 cm^{-1} resolution averaged over 100 scans using a Bruker Vertex 70 spectrometer. XPS analyses were conducted using a PHI 5000 VersaProbe and SEM images were collected using a Hitachi S4800 FE-SEM. Nafion and Teflon AF solutions were obtained from Sigma-Aldrich and Dupont, respectively, and were individually spin coated on Si ⟨100⟩ substrate using Laurell manual spin processor.

Top IR spectrum in Figure 1a represents as-deposited MFP film (~28 nm) on 90 nm low- *k* trench structures. Two broad absorption bands can be seen between 1000 and 1900 cm^{-1}. The dominant absorption bands centered ca. 1233 cm^{-1} were previously identified, by reductive etching using naphthalenide radical anion, to originate from saturated C−F backbone within MFP framework.[9,12] The main IR absorption peak at ~1230 cm^{-1} was assigned to asymmetric CF_2 stretching mode while the broad shoulder on lower wavenumber side was assigned to symmetric CF_2 stretching (~1180 cm^{-1}). Higher wavenumber shoulders were assigned to overlapping terminal CF_3 and branching CF stretching modes. These cross-linked fluoropolymer backbone was decorated by scattered unsaturated bonds (including C═O, C═CF, FC═CF, F_2C═C, F_2C═CF and C═C) formed via radical coupling on the fluorocarbon chain during MFP deposition from fluorohydrocarbon plasma precursors. As shown in Figure 1a, the unsaturated bonds exhibit a broad overlapping absorption band in the range 1500−1850 cm^{-1}.[9,12]

Figure 1a shows that progressive UV irradiations (10−300 s) in atmospheric condition increasingly reduce MFP absorption bands both in intensity and width. Interestingly there was an increased IR band at ~1752 cm^{-1} assigned to C═O groups within the product formed (see mechanism in later section) during early stages of UV/air treatment. The observed blue shift (~30−40 cm^{-1}) compared to a typical C═O vibration frequency suggests *α*-fluoro substitution in carbonyl bonding structures (F_xC═O, *x* = 1−2).[13,14] After 300 s of UV/air exposure, the unsaturated CF_x═CF_y/C═O broad band significantly decayed in corroboration with the decrease of

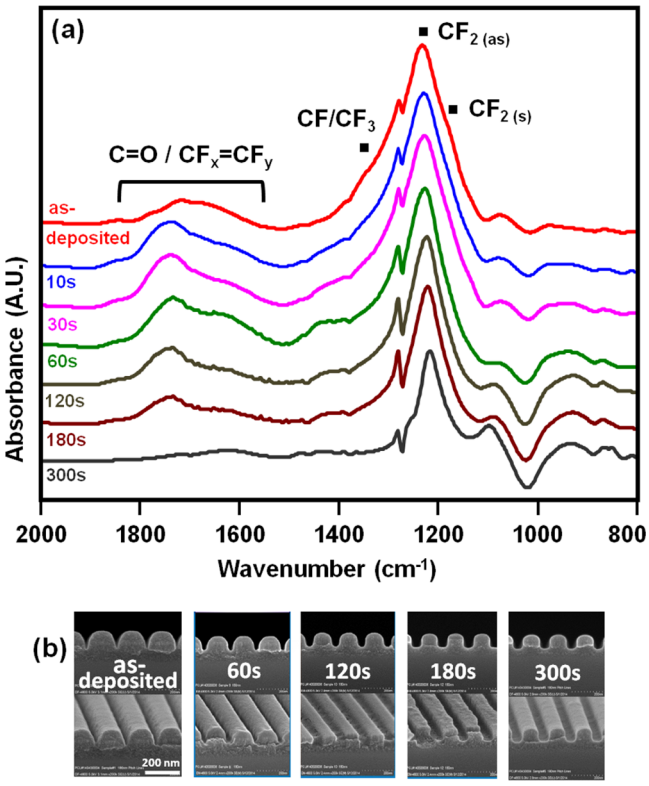

Figure 1. (a) Transmission IR (T-IR) spectra of ~28 nm as-deposited and progressively UV- treated MFP films measured with respect to trench patterned CDO background (before MFP deposition). as = asymmetric; s = symmetric; *x*, *y* = 0−2; no baseline correction. (b) Cross-sectional and top-view SEM images (all in same scale) also support progressive material removal by UV treatment.

main CF_2 band. In addition, progressive modification of low-*k* dielectric with UV irradiations can be seen as negative IR absorption bands at ~1024 cm^{-1} (see Figure 2a and text in later section). SEM images (Figure 1b) confirmed progressive material loss from MFP films with increasing UV irradiation duration. Decreases in fluorine content and oxygen incorporation were also confirmed by comparing average XPS atomic % concentrations from as-deposited (C 57.9%, F 27.3%, O 11.8%) and 300 s UV/air irradiated (C 32.9%, F 23.2%, O 32.9%) MFP films (see the Supporting Information, Figure S2 and Table S1).

All UV-treated samples were subjected to a semiaqueous cleaning step to explore the effect of fluoropolymer removal after UV irradiation. Figure 2a shows differential IR spectra (each subtracted from as-deposited MFP spectrum) of four UV-only and five UV/wet-clean-treated MFP samples. FTIR is a very effective tool to decipher chemical bonding transformations taking place after each processing step. Downward IR absorption bands represent bonds removed by UV/clean process and similarly positive IR bands correspond to bonds formed during UV/clean process and/or queue time. As early as 10 s of UV irradiation (top spectrum in Figure 2a), *α*-fluoro substituted carbonyls (F_xC═O, ~1752 cm^{-1}) readily formed on UV-modified MFP films. Concurrently, new alcohol functional groups (C−OH), which make UV-modified MFP more hydrophilic, were observed at 1427 cm^{-1} from 10 to 120 s UV irradiation. With follow-up wet clean treatment, progressive MFP removal is clearly evidenced, in Figure 2a, by the characteristic broad band centered at ~1242 cm^{-1} (CF_2

DOI: 10.1021/am508734b
ACS Appl. Mater. Interfaces 2015, 7, 5051−5055

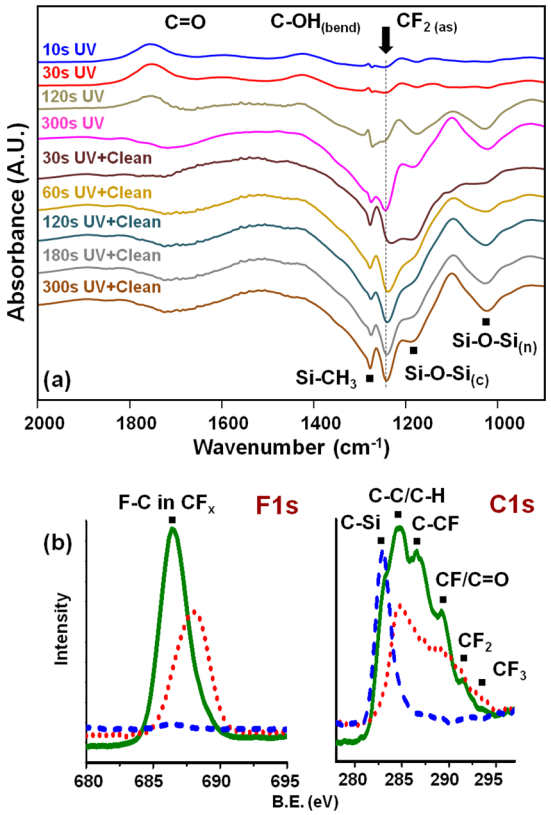

Figure 2. (a) Differential T-IR spectra of selected UV-treated and UV-treated + wet cleaned MFP films. as = asymmetric, c = cage, *n* = network. (b) Comparison of F 1s and C 1s XPS spectra of as-deposited MFP film (green solid line), after 300 s UV/air (red dotted line), and after 300 s UV/air + wet clean (blue dashed line) process.

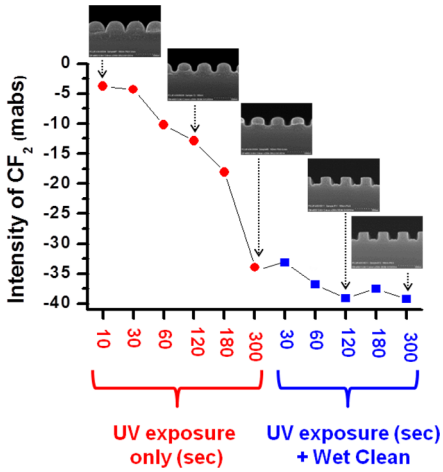

Figure 3. Material removal of model fluorocarbon film (~28 nm) based on observed decrease in CF_2 stretching band at 1242 cm^{-1} during sequential UV/air exposure (solid circles in red) and subsequent wet clean steps (solid squares in blue). Selective SEM cross-sections (insets) show progressively cleaner dielectric trench profile.

asymmetric stretching) and accompanying CF_x═CF_y/C═O band in the range 1500−1850 cm^{-1}. The F 1s core-level XPS spectrum (Figure 2b) confirmed partial fluorine removal after 300s UV/air treatment and total fluorine removal after 300 s UV/air + wet clean step. Complete MFP removal was also substantiated by corresponding C 1s XPS spectra lacking the characteristic CF_n components (C−CF 286.4 eV, CF/C═O 289.2 eV, CF_2 291.5 eV, CF_3 293.8 eV)[9] and consisting of only a narrow band assigned to Si-CH_3 (283 eV) originating from a postclean CDO low-*k* trench structure.

A quantitative assessment of UV-assisted material removal of MFP film was carried out, in Figure 3, based on gradual reduction of main CF_2 asymmetric stretching band at ~1242 cm^{-1}. Interestingly, the amount of fluorocarbon polymer removed during UV/air exposure was higher than the subsequent wet removal according to our IR data. Cross-sectional SEM images (Figure 3 insets) also support progressive material loss. SEM image (300 s UV+Clean, Figure 3 inset) shows a clean vertical etch profile with no observable MFP residues that corroborated well with XPS data to support the complete removal of fluorocarbon etch residues from patterned low-*k* structure.

Therefore, the ≥230 nm UV/air treatment on MFP films was shown to reduce hydrophobic fluorocarbon chain and incorporate O-containing hydrophilic functional groups for better overall MFP removal efficiency in subsequent cleaning solution. However, concomitant damage to the underlying porous low-*k* structure was also observed in the corresponding IR spectra during UV/air exposure and wet removal of the MFP film. For example, the three downward (i.e., chemical bonding loss) absorption band minima in Figure 2a at 1024, 1178, and 1276 cm^{-1}, attributed to Si−O−Si network, Si−O−Si cage, and Si−CH_3 bending vibrations, respectively, suggested low-*k* degradation/modification in each step. Our current observations corroborate well with a recent report[8] of *k* value increase on porous dielectric materials ($k \approx 2.0$) under high UV dose (15 J/cm^2) and >100 Torr oxygen pressure.

In the current study, FTIR, XPS, and SEM data demonstrated that a pretreatment of UV irradiation in air enables the complete removal of ~28 nm MFP film deposited on 90 nm low-*k* dielectric trench lines by subsequent wet clean. The observed photodegradation process required presence of O_2 because UV irradiation in N_2 or vacuum did not show the same removal effect on MFP verified by separate experiments.[8] Considering the chemical bonding structure of MFP coating, fragmentation via direct scission of strong C−F bonds (480−540 kJ/mol)[15] is ruled out because of the low energy UV ($\lambda \geq$ 230 nm) used. To account for the observed morphological changes, we propose the following mechanistic route involving photointeractions between the MFP and incident UV light under atmospheric conditions, summarized in Figure 4a. Initially, MFP film absorbs incident UV light ($\lambda \geq$ 230 nm) via its carbonyl chromophores to form an excited state (MFP*), which then transfers its excess energy to ambient O_2 molecules to generate $^1O_2$. An excited singlet state of O_2 ($^1O_2$) is ~1 V more oxidizing and therefore significantly more electrophilic than its triplet ground state.[16] $^1O_2$ reacts with π bonds in fluoro-substituted olefins embedded in MFP to form 1, 2-dioxetane ring intermediate. Finally the strained four-membered dioxetane ring dissociates to energetically favorable carbonyl products, detected by arisen 1752 cm^{-1} vibrational band. The following section gives detailed consideration of experimental data and reported literatures that support the proposed mechanism.

Photosensitization on saturated chemical bonds (like C−F and C−O) in MFP is not efficient due to high- energy $\sigma \rightarrow \sigma^*$ and n $\rightarrow \sigma^*$ transitions required of a typical polytetrafluoro-ethylene chain that leads to low absorption coefficient (~1 × 10^2 cm^{-1} mol^{-1}) only in far-UV region.[14,17] However, both

DOI: 10.1021/am508734b
ACS Appl. Mater. Interfaces 2015, 7, 5051−5055

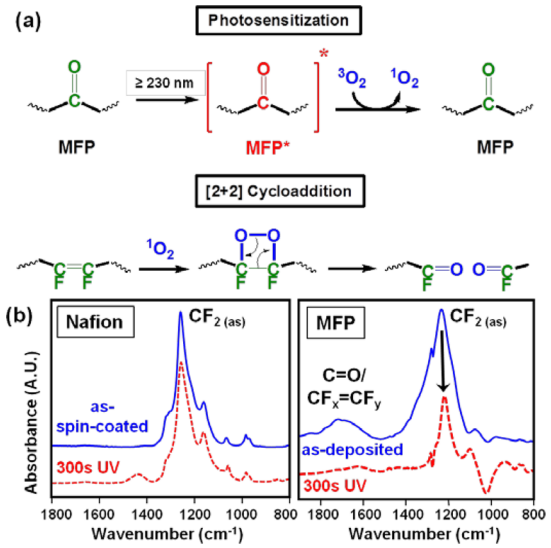

Figure 4. (a) Proposed mechanism of UV-induced photoreaction between fluoropolymer and ambient oxygen molecule. Active carbonyl site in ground state is shown in green fonts and wiggly lines represent nonphotoactive fluorocarbon chain; (b) Comparison of 300 s UV/air treatment on Nafion film (left) and as-deposited model fluoropolymer film (right) supports active participation of unsaturated chromophores in the UV-assisted photodegradation of the irradiated film.

olefin and carbonyl bonds in MFP film can exhibit chromophore properties owing to the possible $\pi \rightarrow \pi^*$ and n $\rightarrow \pi^*$ electronic transitions. Various plasma-polymerized fluorocarbon films were also found to have significant absorption in the >230 nm range attributed to the active chromophores within.[18−21] We propose that the carbonyl chromophore, instead of olefins and C−O proposed previously by Le et al.,[6] play a main role in UV-induced photosensitization mechanism under the current experimental irradiation conditions (≥230 nm UV). Three factors support this assertion: (i) lowest energy absorption bands for typical unconjugated olefins are located <200 nm region, whereas carbonyls absorb >250 nm, (ii) carbonyls display efficient singlet-to-triplet intersystem crossing (ISC) due to higher degree of spin−orbit coupling, (iii) both alkyl-and aryl ketones have been exploited as triplet photosensitizers in chemical and biological reactions.[22,23] As illustrated in Figure 4a, C═O containing MFP is photoexcited by ≥230 nm light to its first singlet excited state via n $\rightarrow \pi^*$ transition, which then interconverts to a triplet excited state. Ambient oxygen (triplet ground state) molecules quench the triplet excite state of C═O and generates a singlet excited state of O_2 ($^3O_2 \rightarrow {}^1O_2$ energy gap ∼94.5 kJ/mol).[23]

Reportedly, singlet oxygen is very long-lived in a fluorocarbon environment, which allows diffusion of $^1O_2$ within the MFP network prior to its decay back to triplet ground state.[24] Synergistically, the π bonds of fluoro-substituted olefins have been shown[25] to be ∼50 kJ/mol weaker than that of regular olefins. The $^1O_2$ acts as a strong oxidizing electrophile to attack the weaker CF_x═CF_y linkages in MFP to form strained, four-membered 1, 2-dioxetane ring intermediate that leads to more stable α-fluoro substituted carbonyls (F_xC═O) products. The overall UV-induced carbonyl formation on MFP film is highly favorable as F_xC═O absorption band at ∼1752 cm^{-1} can be observed as early as 10 s of UV irradiation. Control experiments using two fluoropolymer films were carried out to verify necessity of carbonyls and olefins in the observed photodisintegration phenomenon. Both Nafion (Figure 4b) and Teflon AF (data not shown) fluoropolymer films, lacking C═O chromophores and CF_x═CF_y linkages, did not show significant C−F bond breaking or material removal similar to MFP films after the same 300 s of UV/air treatment. In addition, C−O bonding, as part of Nafion's chemical structure, did not function as chromophore to promote photodisintegration under current irradiation conditions (≥230 nm UV).

With progressive UV exposure, assisted by $^1O_2$, the overall MFP bonding structure is efficiently dissected at where olefin groups are located in its microstructure. When participating olefin groups are parts of side chains in the parent MFP structure, volatile carbonyl products (C_xF_yO, x = 1−4) are formed (see the Supporting Information, Table S2) at the surface temperature (∼50 °C) and released into the ambience that accounts for the progressive reduction of main CF_2 absorption band at 1242 cm^{-1} and accompanying materials loss observed by SEM (Figure 1). In addition, loss of side chains leaves fluoropolymer chain motif in a more ordered state suggested by progressively narrower $CF_{2\ (as)}$ stretching bandwidth (Figure 1a). Although in situ generation of $^1O_2$ by a triplet photosensitizer and its cycloaddition with olefin is frequently encountered in organic reactions,[26] under the studied experimental conditions, formation of other active oxidative species may result in additional secondary reactions leading to fluoropolymer backbone fragmentation. As the UV-induced fragmentation on MFP film proceeds, ambient water molecules can hydrate the fluoro-substituted carbonyl group forming hydroxyl groups, observed as corresponding OH stretching band in >3000 cm^{-1} region films (see the Supporting Information, Figure S3) and OH in-plane bending vibration (1427 cm^{-1} band in Figure 2a). It is important to note that α-fluoro substitution near the electrophilic carbonyl center is known to greatly increase the equilibrium rate constant for water addition reaction.[27] The hydroxyl groups render MFP remnant more hydrophilic and promote efficient removal by subsequent wet clean. FTIR metrology can be utilized to aid the development of less aggressive UV process parameters and improved wet clean formulations with better ILD compatibility.

In summary, using FTIR, XPS and SEM the structural/functional modifications in model fluorocarbon polymer films deposited on manufacturing relevant nanostructured low-k trench patterns were characterized for the first time. Loss of fluorocarbon fragments and incorporation of O-containing hydrophilic functional groups in MFP structure were observed in FTIR and XPS analyses while SEM images revealed progressive MFP material loss on nanotrench structure during UV/air treatment. A subsequent semiaqueous wet clean step further removed remaining UV-modified MFP residues. Essential involvement of unsaturated bonds such as carbonyls and olefins, not C−O bond scisson, in UV-assisted photodegradation process was revealed by control experiments. Synergistic effects of UV light and O_2 molecule was projected as most plausible mechanistic pathway leading to modifications and corporeal loss of MFP mass. On the basis of the observation of concomitant low-k modification by FTIR chemical bonding characterization, further process optimization to minimize UV-induced dielectric damage is ongoing.

■ ASSOCIATED CONTENT

Supporting Information

Experimental procedure details, XPS spectra, and corresponding atomic % of UV-irradiated fluoropolymer films are reported.

DOI: 10.1021/am508734b
ACS Appl. Mater. Interfaces 2015, 7, 5051−5055

IR spectra demonstrating hydroxyl increase in UV- treated fluoropolymer and a list of perfluoro carbonyl compounds with respective boiling points are also shown. This material is available free of charge via the Internet at http://pubs.acs.org.

AUTHOR INFORMATION

Corresponding Author

*E-mail: chyan@unt.edu.

Author Contributions

The manuscript was written through contributions of all authors. All authors have given approval to the final version of the manuscript.

Notes

The authors declare no competing financial interest.

ACKNOWLEDGMENTS

Financial support of this work from Intel and Texas NHARP is gratefully acknowledged. O.C. acknowledges the UNT Center for Advanced Research and Technology (CART) for the help in XPS characterization.

REFERENCES

(1) Baklanov, M.; Green, M.; Maex, K. *Dielectric Films for Advanced Microelectronics*; John Wiley & Sons: Chichester, U.K., 2007.

(2) Baklanov, M. R.; de Marneffe, J.-F.; Shamiryan, D.; Urbanowicz, A. M.; Shi, H.; Rakhimova, T. V.; Huang, H.; Ho, P. S. Plasma Processing of Low-*k* Dielectrics. *J. Appl. Phys.* **2013**, *113*, 041101.

(3) Baklanov, M. R.; Ho, P. S.; Zschech, E. *Advanced Interconnects for ULSI Technology*; John Wiley & Sons: Chichester, U.K., 2012.

(4) Le, Q. T.; de Marneffe, J.-F.; Conard, T.; Vaesen, I.; Struyf, H.; Vereecke, G. Effect of UV Irradiation on Modification and Subsequent Wet Removal of Model and Post-Etch Fluorocarbon Residues. *J. Electrochem. Soc.* **2012**, *159*, H208−H213.

(5) Kesters, K.; Le, Q. T.; Simms, I.; Nafus, K.; Struyf, H.; de Gendt, S. Wet Removal of Post-Etch Residues by a Combination of UV Irradiation and a SC1 Process. *Solid State Phenom.* **2013**, *195*, 114−118.

(6) Le, Q. T.; Naumov, S.; Conrad, T.; Franquet, A.; Müller, M.; Beckhoff, B.; Adelmann, C.; Struyf, H.; de Gendt, S.; Baklanov, M. R. Mechanism of Modification of Fluorocarbon Polymer by Ultraviolet Irradiation in Oxygen Atmosphere. *ECS J. Solid-State Sci. Technol.* **2013**, *2*, N93−N98.

(7) Le, Q. T.; Kesters, E.; Conrad, T.; Struyf, H.; de Gendt, S. UV-induced Modification of Fluorocarbon Polymer: Effect of Treatment Atmosphere and Aging on Dissolution in Organic Solvent. *Solid State Phenom.* **2013**, *195*, 132−135.

(8) Le, Q. T.; Simms, I.; Yue, H.; Brown, I.; Kesters, E.; Vereecke, G.; Struyf, H.; de Gendt, S. UV-induced Modification of Fluorocarbon for Improvement of Subsequent Wet Removal. *Microelectron. Eng.* **2014**, *114*, 136−140.

(9) Mukherjee, T.; Rimal, S.; Koskey, S.; Chyan, O.; Singh, K. J.; Myers, A. M. Bonding Structure of Model Fluorocarbon Polymer Residue Determined by Functional Group Specific Chemical Derivatization. *ECS Solid-State Lett.* **2013**, *2*, N11−N14.

(10) Rimal, S.; Mukherjee, T.; Abdelghani, J.; Goswami, A.; Chyan, O.; Stillahn, J.; Chiba, Y.; Maekawa, K. Evaluation of Plasma Damage to Low-k Dielectric Trench Structures by Multiple Internal Reflection Infrared Spectroscopy. *ECS Solid-State Lett.* **2014**, *3*, N1−N4.

(11) Rimal, S.; Ross, N.; Pillai, K. S. M.; Singh, K. J.; Chyan, O. Characterization of Post Etch Residues on Patterned Porous Low-k Dielectric Using Multiple Internal Reflection Infrared Spectroscopy. *ECS Trans.* **2011**, *41*, 315−322.

(12) Colthup, N. B.; Daley, L. H. *Introduction to Infrared and Raman Spectroscopy*, 3rd ed, Academic Press: San Diego, 1990.

(13) Bellamy, L. J. *The Infrared Spectra of Complex Molecules, Vol. 2: Advances in Infrared Group Frequencies*, 2nd ed.; Chapman and Hall: London, 1980.

(14) Rabek, J. F. *Polymer Photodegradation—Mechanisms and Experimental Methods*; Chapman and Hall: London, 1994.

(15) Luo, Y.-R. *Handbook of Bond Dissociation Energies in Organic Compounds*; CRC Press: Boca Raton, FL, 2002.

(16) DeRosa, M. C.; Crutchley, R. J. Photosensitized Singlet Oxygen and its Applications. *Coord. Chem. Rev.* **2002**, *233−234*, 351−371.

(17) Adhi, K. P.; Owings, R. L.; Railkar, T. A.; Brown, W. D.; Malshe, A. P. Femtosecond Ultraviolet (248nm) Excimer Laser Processing of Teflon (PTFE). *Appl. Surf. Sci.* **2013**, *218*, 17−23.

(18) Weber, A.; Pöckelmann, R.; Klages, C.-P. Electrical and Optical Properties of Amorphous Fluorocarbon Films Prepared by Plasma Polymerization of Perfluoro-1,3- dimethylcyclohexane. *J. Vac. Sci. Technol. A* **1998**, *16*, 2120−2024.

(19) Yi, J. W.; Lee, Y. H.; Farouk, B. Low Dielectric Fluorinated Amorphous Carbon Thin Films Grown from C_6F_6 and Ar Plasma. *Thin Solid Films* **2000**, *374*, 103−108.

(20) Huang, K. P.; Lin, P.; Shih, H. C. Structures and Properties of Fluorinated Amorphous Carbon Films. *J. Appl. Phys.* **2004**, *96*, 354−360.

(21) Easwarakhanthan, T.; Beyssen, D.; Le Brizoual, L.; Bougdira, J. Spectroellipsometric Analysis of CHF_3 Plasma-polymerized Fluorocarbon Films. *J. Vac. Sci. Technol. A* **2006**, *24*, 1036−1043.

(22) Carey, F. A.; and Sundberg, R. J. *Advanced Organic Chemistry, Part A: Structure and Mechanisms*, 5th ed, Springer: New York, 2008.

(23) Anslyn, E. V.; Dougherty, D. A. *Modern Physical Organic Chemistry*; University Science Books: Sacramento, CA, 2005.

(24) Lee, P. C.; Rodgers, M. A. J. Kinetic Properties of Singlet Oxygen in a Polymeric Microheterogeneous System. *J. Phys. Chem.* **1984**, *88*, 4385−4389.

(25) Wang, S. Y.; Borden, W. T. Why is the π Bond in Tetrafluoroethylene Weaker Than That in Ethylene? An Ab Initio Investigation. *J. Am. Chem. Soc.* **1989**, *111*, 7283−7285.

(26) Wasserman, H. H.; Murray, R. W. *Singlet Oxygen*; Academic Press: New York, 1979.

(27) Guthrie, J. P. Carbonyl Addition Reactions: Factors Affecting the Hydrate-Hemiacetal and Hemiacetal-Acetal Equilibrium Constants. *Can. J. Chem.* **1975**, *53*, 898−906.

DOI: 10.1021/am508734b
ACS Appl. Mater. Interfaces 2015, 7, 5051−5055